Numerical investigation of isospectral cavities built from triangles

Hua Wu and D. W. L. Sprung
Department of Physics and Astronomy, McMaster University, Hamilton, Ontario, Canada L8S 4M1

J. Martorell
Departamento d'Estructura i Constituents de la Materia, Facultat Física, University of Barcelona, Barcelona 08028, Spain

(Received 25 July 1994)

We present computational approaches as alternatives to a recent microwave cavity experiment by S. Sridhar and A. Kudrolli [Phys. Rev. Lett. **72**, 2175 (1994)] on isospectral cavities built from triangles. A straightforward proof of isospectrality is given, based on the mode-matching method. Our results show that the experiment is accurate to 0.3% for the first 25 states. The level statistics resemble those of a Gaussian orthogonal ensemble when the integrable part of the spectrum is removed.

PACS number(s): 41.20.−q, 05.45.+b, 03.65.Ge, 02.90.+p

I. INTRODUCTION

In a well-known paper, Kac [1] raised the question of whether two isospectral plane domains must actually be isometric. This is popularly phrased as "Can one hear the shape of a drum?" From the physics viewpoint, since the density of states has an asymptotic expansion whose coefficients depend on the area, perimeter, etc., of the cavity, it is clear that at least these properties must be common, but this leaves open the question of whether the two must be identical in all respects. The question has now received a definitive negative answer. Gordon, Webb, and Wolpert, [2] have given simple examples constructed out of seven right triangles which are isospectral, but not isometric.

These particular shapes were subjected to experimental test by Sridhar and Kudrolli [3] and found to give identical spectra to an accuracy of 0.2% on average for the first 25 eigenenergies. In this paper we present accurate numerical results with the mode-matching and finite-difference methods. The agreement between the two kinds of calculation ensures the accuracy of the results. Compared to the experimental spectra, we find differences of order 0.3%.

In addition, a very simple proof of the isospectrality is obtained with the mode-matching method. The wave function transformation from one cavity to the other is put into a simple form. We find that our computed wave function is in good qualitative agreement with the experimental wave function. The level statistics resemble those of a Gaussian orthogonal ensemble (GOE) when a subset of integrable levels are removed.

In Sec. II we outline the mode-matching method for the two cavities. In Sec. III we demonstrate isospectrality analytically. Section IV contains the numerical results and conclusions.

II. THE MODE-MATCHING METHOD

The problem we wish to solve is Helmholtz's equation

$$(\nabla^2 + E)\Psi = 0 \tag{1}$$

in the interior of regions shown in Fig. 1 with Dirichlet conditions on the boundaries. Each cavity consists of seven equal-sided right triangles. Let the length of a short side of a triangle be the unit length d. Since the cavities are made from regular shapes, we can divide them into smaller regions as shown in Fig. 1. We will first concentrate on cavity 1. The five smaller regions are three triangles labeled A, B, and E, and two squares labeled as C and D. We shall write Ψ_{AB}, etc., for wave-function values along the internal boundary lines separating the regions. Then the auxiliary boundary conditions on the smaller regions are conveniently written by expanding these wave functions in the Fourier series

$$\Psi_{AB} = \sum_n A_{1n} \sin \frac{n\pi x}{d} \quad , \tag{2}$$

$$\Psi_{BC} = \sum_n B_{1n} \sin \frac{n\pi (y-d)}{d} \quad , \tag{3}$$

$$\Psi_{CD} = \sum_n C_{1n} \sin \frac{n\pi (y-d)}{d} \quad , \tag{4}$$

$$\Psi_{DE} = \sum_n D_{1n} \sin \frac{n\pi (x-2d)}{d} \quad . \tag{5}$$

Here $A_{1n}, \ldots, D_{1n}$ are mode expansion coefficients, the subscript 1 denotes cavity 1 and the summation over n is

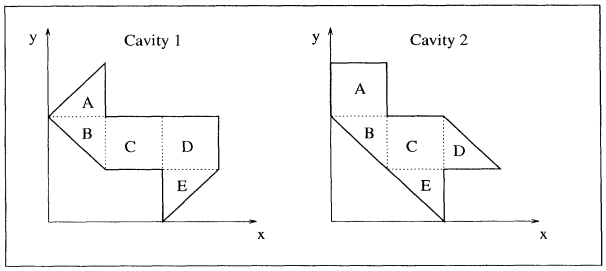

FIG. 1. Geometric shapes of the two two-dimensional domains with identical spectra. The dotted lines are boundary lines dividing the cavities into smaller regions.

from 1 to N, a value truncating the infinite series summation. We shall now see that if these auxiliary boundary conditions are assumed to be known, the wave functions in each region are easily determined as long as the energy does not happen to coincide with an eigenenergy of the small closed region. The wave function for the square region is easy to work out and thanks to the 45° of the triangle, the wave function for the triangle is just that of a square plus antisymmetrization along the diagonal line. Thus

$$\Psi_A = \sum_n A_{1n}\left[\sin\frac{n\pi x}{d}\,\frac{\sin[\alpha_n(3d-y)]}{\sin\alpha_n d} - \sin\frac{n\pi(y-2d)}{d}\,\frac{\sin[\alpha_n(d-x)]}{\sin\alpha_n d}\right] , \quad (6)$$

$$\Psi_B = \sum_n A_{1n}\left[\sin\frac{n\pi x}{d}\,\frac{\sin[\alpha_n(y-d)]}{\sin\alpha_n d} - \sin\frac{n\pi(2d-y)}{d}\,\frac{\sin[\alpha_n(d-x)]}{\sin\alpha_n d}\right] + \sum B_{1n}\left[\sin\frac{n\pi(y-d)}{d}\,\frac{\sin\alpha_n x}{\sin\alpha_n d} - \sin\frac{n\pi(d-x)}{d}\,\frac{\sin[\alpha_n(2d-y)]}{\sin\alpha_n d}\right] , \quad (7)$$

$$\Psi_C = \sum_n B_{1n}\sin\frac{n\pi(y-d)}{d}\,\frac{\sin[\alpha_n(2d-x)]}{\sin\alpha_n d} + \sum_n C_{1n}\sin\frac{n\pi(y-d)}{d}\,\frac{\sin[\alpha_n(x-d)]}{\sin\alpha_n d} , \quad (8)$$

$$\Psi_D = \sum_n C_{1n}\sin\frac{n\pi(y-d)}{d}\,\frac{\sin[\alpha_n(3d-x)]}{\sin\alpha_n d} + \sum_n D_{1n}\sin\frac{n\pi(x-2d)}{d}\,\frac{\sin[\alpha_n(2d-y)]}{\sin\alpha_n d} , \quad (9)$$

$$\Psi_E = \sum_n D_{1n}\left[\sin\frac{n\pi(x-2d)}{d}\,\frac{\sin\alpha_n y}{\sin\alpha_n d} - \sin\frac{n\pi y}{d}\,\frac{\sin[\alpha_n(x-2d)]}{\sin\alpha_n d}\right] , \quad (10)$$

where

$$\alpha_n = \sqrt{E-\left(\frac{n\pi}{d}\right)^2} . \quad (11)$$

By construction, these wave functions are already continuous across the boundary lines. The mode expansion coefficients are now determined by requiring the normal derivatives to be continuous as well. A straightforward calculation gives the condition

$$M_1\begin{bmatrix}A_1\\B_1\\C_1\\D_1\end{bmatrix} = 0 , \quad (12)$$

with

$$M_1 = \begin{bmatrix} U-2W & \overline{W}-\overline{V}/2 & 0 & 0 \\ \overline{W}-\overline{V}/2 & U-W & -V/2 & 0 \\ 0 & -V/2 & U & W \\ 0 & 0 & W & U-\overline{W}\end{bmatrix} , \quad (13)$$

where U,V,W are $N\times N$ matrices with elements defined by

$$U_{m,n} = \delta_{m,n}\alpha_n\cot\alpha_n d , \quad (14)$$

$$V_{m,n} = \delta_{m,n}\alpha_n/\sin\alpha_n d , \quad (15)$$

and

$$W_{m,n} = \frac{(m\pi/d)(n\pi/d)}{E-(m\pi/d)^2-(n\pi/d)^2} . \quad (16)$$

Defining the diagonal matrix P of order N, as $P_{n,n} = (-1)^n$, then

$$\overline{W} = PWP, \quad \overline{V} = PV . \quad (17)$$

In Eq. (12), A_1, etc., are column matrices of order N with A_{1n}, etc., as their elements.

Normally, one would look for nontrivial solutions to Eq. (12) by seeking energies for which $\det(M_1) = 0$. A better way is to diagonalize M_1 first. Then, when scanning in energy a zero eigenvalue is found; this energy corresponds to an eigenmode of the cavity and the corresponding eigenvector gives rise to the wave function. When $\det(M_1) \neq 0$, the wave functions Eqs. (2)–(5) on the internal boundaries vanish and the only possible nontrivial solutions are when the energy coincides with one of the eigenenergies of the smaller regions themselves. Thus, besides the solutions dictated by $\det(M_1) = 0$, other solutions exist at the eigenenergies of the basic triangle, which are known analytically. The wave functions in the several triangles must be in proper phase to make the normal derivatives across the boundary lines continuous and that fixes the relative sign in each small region.

In a totally parallel way, the condition for finding eigenenergies for the second cavity is (see the Appendix)

$$M_2\begin{bmatrix}A_2\\B_2\\C_2\\D_2\end{bmatrix} = 0 \quad (18)$$

with

$$M_2 = \begin{bmatrix} U-W & \overline{W}-\overline{V}/2 & 0 & 0 \\ \overline{W}-\overline{V}/2 & U-W & \overline{V}/2 & W \\ 0 & \overline{V}/2 & U-W & \overline{W} \\ 0 & W & \overline{W} & U-W\end{bmatrix} . \quad (19)$$

The mode-matching method is essentially an analytical one, though it requires numerical diagonalization and root searching. It yields fast convergence with respect to the truncation parameter N. As will be discussed further in the next section, even after truncation the numerical spectra of the two cavities are identical, so that comparing them does not give any additional check on the accuracy of the numerical results. Therefore, as a further check we performed a more conventional calculation using a finite-difference method for the purpose of comparison and testing the results. The implementation is trivial: one replaces the Laplace operator in Eq. (1) with a five point difference formula, and eigenenergies and wave functions are obtained in one single diagonalization step.

III. ISOSPECTRALITY

The theorems proved by Gordon *et al.* [2] ensure that the two cavities have the same spectra. The experimental work of Ref. [3] entailed some error in comparing the two spectra. We shall now discuss how well the numerical computations presented here confirm the isospectrality theorem. With the same grid size, we find that the finite-difference method gives exactly the same spectra (up to machine precision) for the two cavities. Thus, even for a finite grid size, and although the method is an approximation to the real cavities, isospectrality is always precise. The same property holds for the mode-matching method. To prove this, we notice that the matrices M_1 and M_2 are connected by an orthogonal transformation

$$T = \frac{1}{\sqrt{2}} \begin{bmatrix} 0 & 1 & 0 & P \\ 1 & 0 & P & 0 \\ 0 & -1 & 0 & P \\ -1 & 0 & P & 0 \end{bmatrix} , \tag{20}$$

$$M_1 = T^t M_2 T \quad . \tag{21}$$

This proves that the determinants of M_1 and M_2 have the same set of zeros and therefore produce the same spectra. In addition, substituting Eq. (21) into Eq. (12)

$$M_2 T \begin{bmatrix} A_1 \\ B_1 \\ C_1 \\ D_1 \end{bmatrix} = 0 \quad . \tag{22}$$

Thus the wave functions in the two cavities are connected by

$$\begin{bmatrix} A_2 \\ B_2 \\ C_2 \\ D_2 \end{bmatrix} = T \begin{bmatrix} A_1 \\ B_1 \\ C_1 \\ D_1 \end{bmatrix} \quad . \tag{23}$$

This relationship is consistent with Eq. (1) of Ref. [3], but has a more compact and easily accessible form. It is valid for arbitrary truncation number N. By taking $N \to \infty$, we have an alternative proof of the isospectrality of these two cavities, which uses tools more familiar to the physicist. Clearly, the two cavities represent the same quantum problem, but in different representations.

IV. RESULTS AND DISCUSSION

Since our computations yield exactly the same energies for the two cavities, only one spectrum is presented. There is a subset of levels, those of the unit triangle, which are analytically known and these have to be added to the zeros of $\det(M_1)$. Introducing an energy unit $E_u = (\pi/d)^2$, the eigenenergies of a unit square are $(n_x^2 + n_y^2)E_u$. For a unit triangle, due to the antisym-

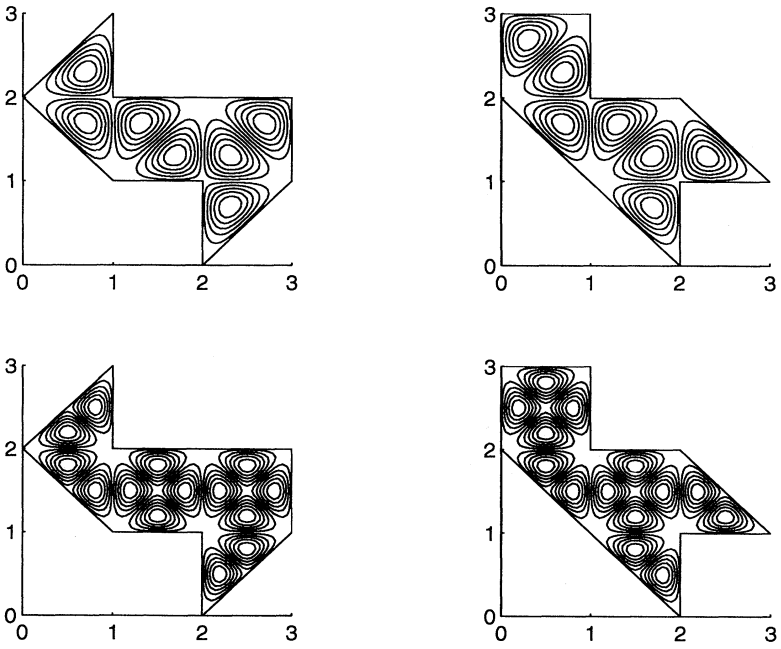

FIG. 2. Contour plot of wave functions for the 9th (the top row) and the 21st (bottom row) states which are eigenstates of a closed unit triangle. The 21st state is exactly the doubling of the 9th state.

metrization requirement, the allowed eigenenergies are the same with the restriction $n_x > n_y$, with corresponding wave function

$$\Psi_{n_x,n_y} = \sin\frac{n_x\pi x}{d}\sin\frac{n_y\pi y}{d} - \sin\frac{n_x\pi y}{d}\sin\frac{n_y\pi x}{d}. \quad (24)$$

The first two such states are at $5E_u$ and $10E_u$, which correspond to modes $(n_x, n_y) = (2,1)$ and $(3,1)$. Compared with the experimental or calculated spectrum, they are the 9th and 21st states. In Fig. 2 we plot these two states, revealing their triangular nature. Because these states are analytically known and are observed experimentally, they can be used to calibrate the experiment.

There are degenerate states within the set of triangular states. The first twofold degenerate pair appears at $E = 65E_u$ with modes (7,4) and (8,1). Aside from the triangular states, numerical results show there are no other degenerate states up to the 600th level.

Table I lists 25 levels from the experiment of Ref. [3] and from our calculation. Column 1 is simply the state sequential number. All the energies are in units of E_u. The second and the third columns (cavities 1 and 2) are obtained from the measured frequencies of Table I of Ref. [3] with the conversion formula $E/E_u = (2fd/c)^2 = 0.25842[f\ (\mathrm{GHz})]^2$. If the experiment were done with air in the cavity as the normal condition, the conversion factor would be multiplied by 1.0006. Table I assumes this situation. These two sets of data agree with an average percentage error 0.2%.

The fourth column (FD) is the result from finite-differences. Calculations for grid sizes $h = d/30$, $d/40$, and $d/50$ were found to vary quadratically with grid size h. Richardson extrapolation to the limit gives accurate eigenvalues.

The last column (MM) is the result from our mode-matching method. Results were found to vary linearly in the variable $1/N$. Values from $N = 50$ and $N = 60$ were extrapolated linearly to $N \to \infty$. Comparing FD with MM, the error is 0.02%. This small error probably comes primarily from the finite-difference method. Comparing the mode-matching method with either cavity's experimental data shows the difference is 0.3% on average. Thus the two computational results agree by one order of magnitude better than the agreement between theory and experiment. Figure 3 shows the error as compared with the average level spacing (dE), relative to

TABLE I. The first 25 eigenvalues from the experiment of Ref. [3] and from our finite-difference and mode-matching numerical calculations.

n	Cavity 1	Cavity 2	FD	MM
1	1.02471	1.02481	1.0289358	1.0285350
2	1.46899	1.47194	1.4818654	1.4814672
3	2.08738	2.08831	2.0982494	2.0974674
4	2.64079	2.63985	2.6497154	2.6495466
5	2.93297	2.92949	2.9381762	2.9374335
6	3.72675	3.71892	3.7326894	3.7323341
7	4.28393	4.28388	4.2951927	4.2947278
8	4.67021	4.66917	4.6776652	4.6775322
9	4.98838	4.98531	5.0000019	5.0000000
10	5.27908	5.27278	5.2914753	5.2902751
11	5.78755	5.78371	5.8015308	5.8011384
12	6.41357	6.43781	6.4338942	6.4321556
13	6.84891	6.84718	6.8662601	6.8662262
14	7.15242	7.16045	7.1598024	7.1593432
15	7.67783	7.70604	7.6947374	7.6924171
16	8.44285	8.45947	8.4636545	8.4632568
17	8.57859	8.62220	8.6135359	8.6111689
18	8.99495	8.97209	9.0124054	9.0103493
19	9.60312	9.59562	9.6099682	9.6097908
20	9.92583	9.93689	9.9211311	9.9210396
21	10.00330	10.03932	10.0000076	10.0000000
22	10.55227	10.55740	10.5710201	10.5697365
23	11.09578	11.10035	11.0669165	11.0657272
24	11.41874	11.40569	11.4195509	11.4188499
25	11.99364	11.98033	11.9846497	11.9840803

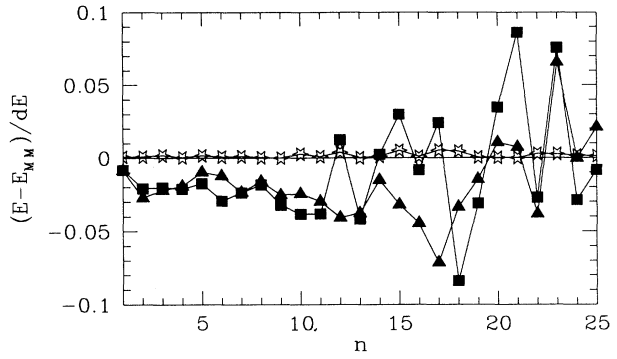

FIG. 3. Error relative to the mode-matching method as compared to the average level spacing dE. Finite-difference method (stars); experimental values: cavity 1 (triangles) and cavity 2 (squares).

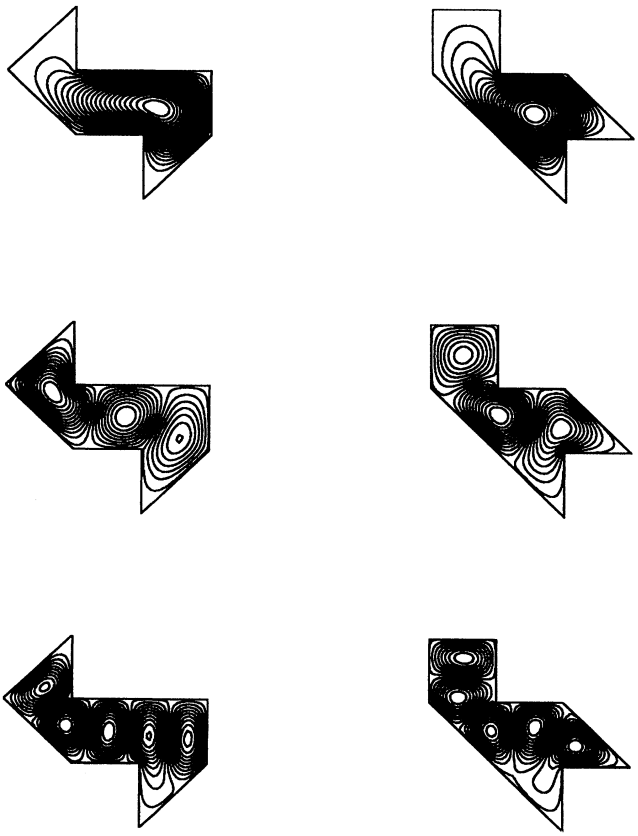

FIG. 4. Contour plot of the wave functions for states 1, 3, and 6, which correspond to the measured wave functions in Fig. 2 of Ref. [3].

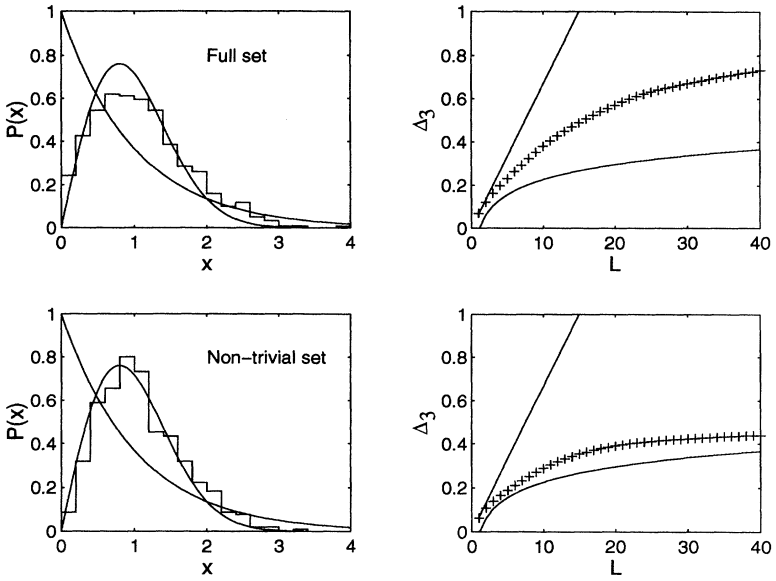

FIG. 5. Nearest level spacing distribution $P(X)$ and Δ_3 statistics of the spectrum. The upper panel is for the full set of the first 598 states. The bottom panel is after the 78 triangular states were removed. Also plotted are Wigner and Poisson distribution curves.

the mode-matching method $[(E - E_{\mathrm{MM}})/dE]$. It reveals both statistical and systematic error in the data. The error is confined within 10% margin of the average level spacing. On average, the root mean square of this quantity is 3% for cavity 1, 4% for cavity 2, and 0.2% for the finite-difference calculation.

One of the highlighted points of Ref. [3] was the ability to measure the wave function. Figure 4 plots the first, third, and sixth wave functions, which show qualitative agreement with experiment. Our more accurate wave functions may be useful in further study on the problem of classical quantum correspondence.

We computed the level statistics for the first 598 states as shown in Fig. 5. The actual spectrum was unfolded using the average density of states obtained from Weyl's formula as given by Ref. [3]. However, we corrected the topological constant to be 5/12 rather than the stated 0.54. One sees excellent agreement with the quantum spectrum. Because each cavity is a pseudointegrable system [4], the statistics are closer to a GOE than to Poisson. As we have pointed out, there are degeneracies among the triangular eigenstates; this part of the spectrum is fully integrable. Among the first 598 states, there are 78 such triangular states. Separating them from the whole spectrum, the level statistics of the remainder are now very much like that of a GOE, a type of level statistics often associated with nonintegrable systems [5].

In summary, we have presented numerical calculations for the isospectral problem in domains constructed from right angle 45° triangles. We found accurate theoretical results which confirm the experiment and give an absolute reference to the data. We point out a subset of eigenstates which are analytically solvable and can be used to calibrate the experiment. The mode-matching method also yields a simple analytical proof of isospectrality.

ACKNOWLEDGMENTS

We are grateful to NSERC Canada for continued support under research Grant No. OGP00-3198 (D.W.L.S. and H.W.). The work of J.M. is supported under Grant No. PB91-0236 of DGICYT, Spain.

APPENDIX: MODE MATCHING FORMULA FOR CAVITY 2

The auxiliary boundary values are expanded as

$$\Psi_{AB} = \sum_n A_{2n} \sin \frac{n\pi x}{d} \quad , \tag{A1}$$

$$\Psi_{BC} = \sum_n B_{2n} \sin \frac{n\pi (y-d)}{d} \quad , \tag{A2}$$

$$\Psi_{CD} = \sum_n C_{2n} \sin \frac{n\pi (2d-y)}{d} \quad , \tag{A3}$$

$$\Psi_{CE} = \sum_n D_{2n} \sin \frac{n\pi (x-d)}{d} \quad . \tag{A4}$$

Then

$$\Psi_A = \sum_n A_{2n} \sin \frac{n\pi x}{d} \frac{\sin[\alpha_n (3d-y)]}{\sin \alpha_n d} \quad , \tag{A5}$$

$$\begin{aligned} \Psi_B = \sum A_{2n} \Bigg[& \sin \frac{n\pi x}{d} \frac{\sin[\alpha_n (y-d)]}{\sin \alpha_n d} \\ & - \sin \frac{n\pi (2d-y)}{d} \frac{\sin[\alpha_n (d-x)]}{\sin \alpha_n d} \Bigg] \\ + \sum_n B_{2n} \Bigg[& \sin \frac{\sin n\pi (y-d)}{d} \frac{\sin \alpha_n x}{\sin \alpha_n d} \\ & - \sin \frac{n\pi (d-x)}{d} \frac{\sin[\alpha_n (2d-y)]}{\sin \alpha_n d} \Bigg] \quad , \end{aligned} \tag{A6}$$

$$\Psi_C = \sum_n B_{2n} \sin\frac{n\pi(y-d)}{d}\,\frac{\sin[\alpha_n(2d-x)]}{\sin\alpha_n d} + \sum_n C_{2n} \sin\frac{n\pi(2d-y)}{d}\,\frac{\sin[\alpha_n(x-d)]}{\sin\alpha_n d} + \sum_n D_{2n} \sin\frac{n\pi(x-d)}{d}\,\frac{\sin[\alpha_n(2d-y)]}{\sin\alpha_n d} \quad , \tag{A7}$$

$$\Psi_D = \sum_n C_{2n}\left[\sin\frac{n\pi(2d-y)}{d}\,\frac{\sin[\alpha_n(3d-x)]}{\sin\alpha_n d} - \sin\frac{n\pi(x-2d)}{d}\,\frac{\sin[\alpha_n(y-d)]}{\sin\alpha_n d}\right] \quad , \tag{A8}$$

$$\Psi_E = \sum_n D_{2n}\left[\sin\frac{n\pi(x-d)}{d}\,\frac{\sin\alpha_n y}{\sin\alpha_n d} - \sin\frac{n\pi(d-y)}{d}\,\frac{\sin[\alpha_n(2d-x)]}{\sin\alpha_n d}\right] \quad . \tag{A9}$$

Matching normal derivatives

$$\int_0^d \sin\frac{m\pi x}{d}\left[\frac{\partial\Psi_B}{\partial y} - \frac{\partial\Psi_A}{\partial y}\right]_{y=2d} = 0 \quad , \tag{A10}$$

$$\int_d^{2d} \sin\frac{m\pi(y-d)}{d}\left[\frac{\partial\Psi_B}{\partial x} - \frac{\partial\Psi_C}{\partial x}\right]_{x=d} = 0 \quad , \tag{A11}$$

$$\int_d^{2d} \sin\frac{m\pi(y-d)}{d}\left[\frac{\partial\Psi_C}{\partial x} - \frac{\partial\Psi_D}{\partial x}\right]_{x=2d} = 0 \quad , \tag{A12}$$

$$\int_d^{2d} \sin\frac{m\pi(x-d)}{d}\left[\frac{\partial\Psi_C}{\partial y} - \frac{\partial\Psi_E}{\partial y}\right]_{y=d} = 0 \quad . \tag{A13}$$

Allowing m to run from 1 to N, Eqs. (A10)–(A13) give rise to Eq. (18).

[1] M. Kac, Am. Math. Mon. **73**, Pt. II, 1 (1966).
[2] C. Gordon, D. Webb, and S. Wolpert, Invent. Math. **110**, 1 (1992).
[3] S. Sridhar and A. Kudrolli, Phys. Rev. Lett. **72**, 2175 (1994).
[4] P. J. Richens and M. V. Berry, Physica D **2**, 495 (1981).
[5] O. Bohigas, M. J. Giannoni, and C. Schmit, Phys. Rev. Lett. **52**, 1 (1984).